Performance Improvement of Very Short-term Prediction Intervals for Regional Wind Power Based on Composite Conditional Nonlinear Quantile Regression

Yan Zhou, Yonghui Sun, Sen Wang, Rabea Jamil Mahfoud, Hassan Haes Alhelou, *Senior Member*, *IEEE*, Nikos Hatziargyriou, *Fellow*, *IEEE*, and Pierluigi Siano, *Senior Member*, *IEEE*

***Abstract*—Accurate regional wind power prediction plays an important role in the security and reliability of power systems. For the performance improvement of very short-term prediction intervals (PIs), a novel probabilistic prediction method based on composite conditional nonlinear quantile regression (CCNQR) is proposed. First, the hierarchical clustering method based on weighted multivariate time series motifs (WMTSM) is studied to consider the static difference, dynamic difference, and meteorological difference of wind power time series. Then, the correlations are used as sample weights for the conditional linear programming (CLP) of CCNQR. To optimize the performance of PIs, a composite evaluation including the accuracy of PI coverage probability (PICP), the average width (AW), and the offsets of points outside PIs (OPOPI) is used to quantify the appropriate upper and lower bounds. Moreover, the adaptive boundary quantiles (ABQs) are quantified for the optimal performance of PIs. Finally, based on the real wind farm data, the superiority of the proposed method is verified by adequate comparisons with the conventional methods.**

***Index Terms*—Regional wind power, probabilistic prediction, nonlinear quantile regression, composite evaluation, adaptive boundary quantiles.**

NOMENCLATURE

η	Indicator of quantile
$\bar{\xi}$, $\underline{\xi}$, $\bar{\psi}$, $\underline{\psi}$	Auxiliary variables
λ_D	Weight of dynamic difference
λ_T	Weight of static difference
λ_ω	Weight of meteorological difference
υ	Difference between adjacent explanatory variables
ω	Wind speed in numerical weather prediction (NWP)
α	Nominal proportion of prediction intervals (PIs)
$\bar{\alpha}$	Nominal proportion of upper quantile
$\underline{\alpha}$	Nominal proportion of lower quantile
AW_α	Average width of PIs with α
$\lvert ACE \rvert$	Absolute value of proportion deviation
C	Correlation coefficient
Cap	Wind farm capacity
D_D	Distance of dynamic difference
D_T	Distance of static difference
D_{WMTSM}	Distance of weighted multivariate time series motifs (WMTSM)
D_ω	Distance of meteorological difference
F	Composite optimization considering offsets of points outside PIs (OPOPI), sharpness, and reliability
g	Output function of extreme learning machine (ELM)
i, j, m, n	Common indices
I_α	PI in a time point with α
IS_α	Interval score with α
k	Spearman correlation coefficient
K	Weighting coefficient
M	Number of wind farms
N	Number of input variables in each sample
$q_{\bar{\alpha}}$	Upper quantile of PI with $\bar{\alpha}$
$q_{\underline{\alpha}}$	Lower quantile of PI with $\underline{\alpha}$

Manuscript received: December 17, 2020; revised: April 2, 2021; accepted: August 6, 2021. Date of CrossCheck: August 6, 2021. Date of online publication: October 22, 2021.

This work was supported by the National Key R&D Program of China "Technology and Application of Wind Power/Photovoltaic Power Prediction for Promoting Renewable Energy Consumption" (No. 2018YFB0904200) and Complement S&T Program of State Grid Corporation of China (No. SGLNDKOOKJJS1800266).

Y. Zhou, Y. Sun (corresponding author), S. Wang, and R. J. Mahfoud are with the College of Energy and Electrical Engineering, Hohai University, Nanjing 210098, China (e-mail: zhouyan@hhu.edu.cn; sunyonghui168@gmail.com; senwang@hhu.edu.cn; rabea7mahfoud@hotmail.com).

H. H. Alhelou is with the Department of Electrical Engineering, Tishreen University, Latakia 2230, Syria (e-mail: h.haesalhelou@gmail.com).

N. Hatziargyriou is with the National Technical University of Athens, Athens 15773, Greece (e-mail: nh@power.ece.ntua.gr).

P. Siano is with the Department of Management & Innovation Systems, University of Salerno, Salerno 84084, Italy (e-mail: psiano@unisa.it).

DOI: 10.35833/MPCE.2020.000874

S_α	Score in a time point with α
t	Wind power observation
T_p	Number of testing samples
T	Number of training samples
w	Output weight of ELM
W	Width of PI
x	Input variable of ELM
$\boldsymbol{x}^*$	Explanatory variable vector
$\boldsymbol{X}$	Matrix consisting of input variables in training samples
y	Prediction target of training sample
$\boldsymbol{Y}$	Output vector of training samples

I. Introduction

With the increasing capacity of renewable energy, the randomness and dynamic fluctuations of electrical magnitudes set new requirements for power system security, efficiency, and flexibility [1]-[3]. More specifically, as wind power production usually suffers from lower controllability and higher variability, compared with conventional power generation, considerable uncertainties in power system operation are introduced [4], [5]. The very short-term wind power prediction within a few hours is therefore of primary importance in order to derive a dispatching plan that maintains a high-level reliability and reduces the operation cost of the power system [6], [7].

Based on the result of point prediction, prediction intervals (PIs) can be utilized for quantification of uncertainties within prescribed confidence level [8], [9]. In [10], PIs were quantified based on point prediction and conditional probability considering Gaussian distribution. In [11], a bootstrap-based extreme learning machine (BELM) was applied to quantify PIs. As analyzed in [12], the performance of the parametric methods was directly affected by the accuracy of error assumption. Thereafter, the nonparametric PIs should be considered. Linear quantile regression (LQR) was proposed for nonparametric PIs efficiently, which directly quantifies the boundary quantiles as bounds [13]. To improve the forecasting performance, the nonlinear quantile regression (NQR) combining extreme learning machine (ELM) and LQR was proposed [14]. ELM makes the inputs nonlinear for better regression analysis. In addition, due to the high efficiency of ELM which is a feed-forward neural network, the NQR ensures both accuracy and efficiency based on linear programming (LP). In [15], coefficient penalty and sensitivity analysis were applied to improve the performance of quantile regression (QR) based method. The sensitivity analysis was performed to quantify the optimized sharpness for the improved overall performance. However, overall performance includes not only the reliability and sharpness, but also the offsets of points outside PIs (OPOPI) [11]. Hence, it is necessary to incorporate OPOPI into the objective function to optimize the boundary quantiles. Besides, to improve the robustness and flexibility of PIs, the nominal proportions of boundary quantiles should be optimized, rather than the fixed nominal proportions in the conventional QR based method, which are symmetric on both sides of the median nominal proportion.

With the clustering algorithm of numerical weather prediction (NWP), the similarity of samples was used to improve the accuracy of point prediction [16], [17]. In [18], a self-organized map (SOM) was applied to cluster the inputs based on weather stability, the uncertainty of point prediction model and NWP. Then, radial basis function neural networks (RBFNNs) were used for the predictions with high reliability. In [19], PV power forecasting accuracy based on RBFNN was improved by clustering considering the variable importance. In [20], data were divided into nonlinear parts of wind power by SOM. Based on a novel fuzzy clustering method, the periodicities of load time series were studied in [21]. The clustering techniques described in [19]-[21] improved the accuracy of model construction. The conventional clustering-based methods quantified the similarity or distance to obtain the appropriate samples for training, and removed the samples with low correlation to improve the performances of the deterministic prediction and related PIs [10], [16], [17]. To further enhance the accuracy of samples' utilization, all samples should be weighted. That is, samples with high correlation have a noticeable influence, while the samples with low correlation have a small influence. By weighting training samples, all their information is taken into account to avoid the missing of sample information for the QR-based nonparametric PIs, which directly quantifies the output coefficients based on optimal performance of PIs.

The above-mentioned methods were applied for power prediction of a single wind farm. For the dispatching function, however, the significance of regional power prediction is much higher than that of a single wind farm. In [22] and [23], NWP and spatial distribution were combined to analyze the regional wind power generation. In [24], according to the correlation between the output of a single wind farm and that of the cluster, and the accuracy of the point prediction, representative wind farms were selected and their weights were quantified. To further improve the accuracy of regional output prediction, the analysis of spatio-temporal correlation (STC) was performed [25]. Markov chain-based algorithm via graphical spatio-temporal learning-based model was used in [26]. In general, the temporal correlation reflects the time series characteristics of the single wind farm generation or the regional generation, and at the same time, the spatial correlation reflects the changes in similarity and synchronicity of generations of wind farms. In [27], the smoothing effect of regional wind power output was considered. The prediction method of regional wind power based on wind speed was proposed by weighting the STC of historical sampling points. The wind speeds of several wind farms were used to quantify the spatial correlation at a given moment, and the time interval between the observations and the outputs to be predicted was used to quantify the temporal correlation. The wind speed at the time of prediction obtained from NWP was used to cluster the wind power or quantify the correlation of wind farms [28]. In [29], the changing trend of time series was used to cluster the inputs.

In this way, the process of power time series can be represented, although a simple trend is frequently not enough, and the magnitude of fluctuation would be needed. Besides, similarity analysis should be also based on the weighted variables in subsequences. Therefore, a clustering analysis weighting dynamic similarity, static similarity, and meteorological similarity appears to be highly promising.

Hence, based on the aforementioned literature, a probabilistic prediction method of very short-term PIs for regional wind power based on composite conditional nonlinear quantile regression (CCNQR) is proposed in this paper, with the following main contributions:

1) A hierarchical clustering method based on weighted multivariate time series motifs (WMTSM) is used to analyze the static characteristic, dynamic characteristic and meteorological characteristic of regional wind power.

2) Based on the clustering analysis, the correlation coefficients are formulated as the weights for the accuracy of samples' utilization used to optimize the cost function of conditional LP (CLP). In addition, to further improve the performance of PIs, the composite evaluation by considering reliability, sharpness, and OPOPI, combined with the adaptive boundary quantiles (ABQs) is studied.

The rest of the paper is organized as follows. In Section II, the proposed WMTSM and CLP are described. Besides, combined with the ABQs, composite optimization considering reliability, average width (AW), and OPOPI is presented. The model construction process is demonstrated in Section III. Case studies are presented in Section IV, which illustrate the effectiveness of the proposed method. Conclusions are drawn in Section V.

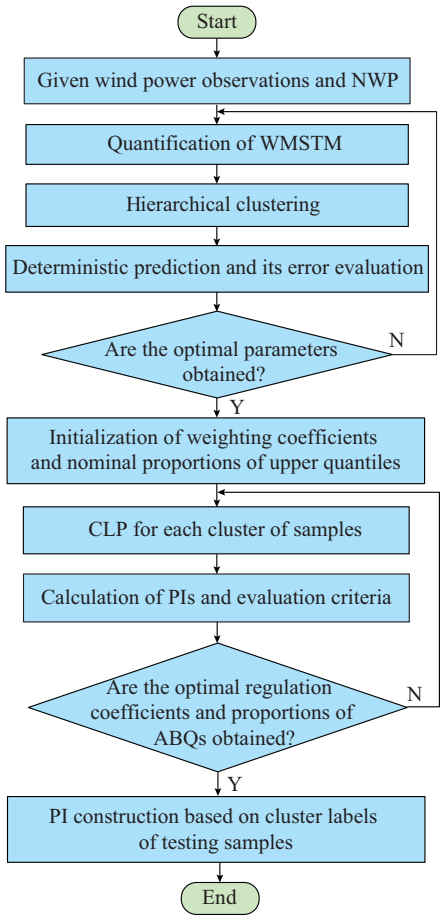

Fig. 1. Flowchart of proposed method.

II. Proposed Methodologies

The flowchart of the proposed method is illustrated in Fig. 1, which has three primary methodologies, including the WMSTM-based clustering, CLP, and composite optimization considering ABQs.

A. Analysis of WMTSM

To improve the accuracy of hierarchical clustering by calculating the similarity based on Euclidean distance [30], not only the wind speed in NWP, but also the process and fluctuation of wind generation should be considered. In the hierarchical clustering method based on WMTSM, the dynamic difference is quantified based on the variation of wind power time series, while the static distance is quantified based on the regional wind power time series, and the meteorological distance is quantified based on the wind speed. The correlations between input variables and output variables are also considered.

The process of WMTSM for sample distance is listed as follows.

1) According to the regional wind power time series, the matrix $\boldsymbol{X}$ is defined as:

$$\boldsymbol{X}=\begin{bmatrix} x_{1,1} & x_{1,2} & \cdots & x_{1,T} \\ x_{2,1} & x_{2,2} & \cdots & x_{2,T} \\ \vdots & \vdots & & \vdots \\ x_{N,1} & x_{N,2} & \cdots & x_{N,T} \end{bmatrix} \tag{1}$$

2) Due to the complex correlation between the input variables and output variables, the Spearman correlation analysis can be utilized to quantify the correlation between $\boldsymbol{x}^*(i)$ and $\boldsymbol{Y}$ [31], [32]. $\boldsymbol{x}^*(i)$ is defined as:

$$\boldsymbol{x}^*(i)=[x_{i,1} \quad x_{i,2} \quad \ldots \quad x_{i,T}] \tag{2}$$

3) For the m^{th} input vector $[x_{m,1}, x_{m,2}, \ldots, x_{m,N}]$, the difference between the adjacent explanatory variables represented by $[\upsilon_{m,1}, \upsilon_{m,2}, \ldots, \upsilon_{m,N-1}]$ is utilized to quantify the fluctuation of adjacent variables. $\upsilon_{m,i}$ is defined as:

$$\upsilon_{m,i}=x_{m,i+1}-x_{m,i} \quad i=1,2,\ldots,N-1 \tag{3}$$

4) Based on the above analysis, the distance of WMTSM between the m^{th} input vector and the n^{th} input vector is formulated as:

$$D_T=\sqrt{\sum_{i=1}^{N} k_i^2 (x_{m,i}-x_{n,i})^2} \tag{4}$$

$$D_D=\sum_{j=1}^{N-1}[(k_i+k_{i+1})(\upsilon_{m,j}-\upsilon_{n,j})]^2 \tag{5}$$

$$D_\omega=\sum_{i=1}^{M} Cap_i \cdot \left|\omega_m-\omega_n\right| \tag{6}$$

$$D_{WMTSM}=\lambda_T D_T+\lambda_D D_D+\lambda_\omega D_\omega \tag{7}$$

The hierarchical clustering method based on WMTSM aims at weighting D_T, D_D, and D_ω to quantify the distances between samples. Cap_i can be used as the weighting coeffi-

cient of wind speed for each wind farm in the regional wind farms [27]. λ_T, λ_D, and λ_ω are optimized to balance different characteristics according to the accuracy of deterministic prediction. k_i is used to consider the importance of input variables and their effect on output differently. That is, the input variables with higher correlations play a greater role in clustering of input vectors than those with lower correlations to enhance the effectiveness of clustering. The quantification of the WMTSM distance leads to the hierarchical clustering method.

With WMSTM analysis, the correlation of samples C is defined as:

$$C = \exp(-D_{WMSTM}) \tag{8}$$

B. Conditional NQR

In NQR [14], the output weights are optimized by LP to minimize the cost function. All training samples are equally weighted. Herein, to weight the samples in training of each cluster, CLP for output weights of one cluster is obtained from

$$\min_{w_\alpha, \bar{\xi}_{i,\alpha}, \underline{\xi}_{i,\alpha}} \sum_{\alpha \in \{\underline{\alpha}, \bar{\alpha}\}} \sum_{i=1}^{T} C_i \left[\alpha \bar{\xi}_{i,\alpha} + (1-\alpha) \underline{\xi}_{i,\alpha} \right] \tag{9}$$

s.t.

$$g(x_i, w_{\underline{\alpha}}) - g(x_i, w_{\bar{\alpha}}) \le 0 \quad \forall i \tag{10}$$

$$0 \le g(x_i, w_\alpha) \le 1 \quad \forall \alpha, \forall i \tag{11}$$

$$\begin{cases} \bar{\xi}_{i,\alpha} \ge 0 \\ \underline{\xi}_{i,\alpha} \ge 0 \end{cases} \quad \forall \alpha, \forall i \tag{12}$$

$$-\underline{\xi}_{i,\alpha} \le y_i - g(x_i, w_\alpha) \le \bar{\xi}_{i,\alpha} \quad \forall \alpha, \forall i \tag{13}$$

In CLP, different correlations are utilized for the samples from different clusters. Meanwhile, the samples with low correlations are also considered, instead of being simply removed. Comprehensive use of the samples with weighting coefficients is studied to improve the accuracy of samples' utilization. The magnitude of influence is directly determined by the correlations which are quantified by calculating the distances between the cluster centers.

C. Performance Optimizations of PIs

The performance of PIs is evaluated considering both reliability and overall performance based on the deviation $|ACE|$ between the PI coverage probability (PICP) and PI nominal confidence (PINC), and the interval score, respectively [11]. The PICP is defined as:

$$PICP = \frac{1}{T_p} \sum_{i=1}^{T_p} \eta_i \tag{14}$$

$$\eta_i = \begin{cases} 1 & t_i \in I_\alpha \\ 0 & t_i \notin I_\alpha \end{cases} \tag{15}$$

The sharpness is defined as:

$$AW_\alpha = \sum_{i=1}^{T_p} W(x_i) \tag{16}$$

$$W(x_i) = q_{\bar{\alpha}}(x_i) - q_{\underline{\alpha}}(x_i) \tag{17}$$

To comprehensively evaluate the performance of PIs including the sharpness, the interval score [10] - [15], [33] is formulated as:

$$S_\alpha(x_i) = \begin{cases} -2(1-\alpha)W(x_i) - 4(q_{\underline{\alpha}}(x_i) - t_i) & t_i < q_{\underline{\alpha}}(x_i) \\ -2(1-\alpha)W(x_i) & t_i \in I_\alpha(x_i) \\ -2(1-\alpha)W(x_i) - 4(t_i - q_{\bar{\alpha}}(x_i)) & t_i > q_{\bar{\alpha}}(x_i) \end{cases} \tag{18}$$

$$IS_\alpha = \frac{1}{T_p} \sum_{i=1}^{T_p} S_\alpha(x_i) \tag{19}$$

As analyzed above, the interval score is a significant criterion for the overall performance of PIs. In (19), the interval score is quantified by the average score of all PIs. As shown in (18), when the actual points are outside the PIs, the larger the actual point deviating from PIs, the lower the score. Thus, to evaluate the overall performance, not only the reliability and sharpness, but also the OPOPI should be considered in the cost function of model training. The cost function of CCNQR based on CLP and composite optimization is described as (20), whose constraints contain (10)-(13) and (21)-(28).

$$\min_{\bar{\xi}_{i,\alpha}, \underline{\xi}_{i,\alpha}, \bar{\psi}_i, \underline{\psi}_i, w_\alpha} \sum_{\alpha \in \{\underline{\alpha}, \bar{\alpha}\}} \sum_{i=1}^{T} \left\{ C_i \left[\alpha \bar{\xi}_{i,\alpha} + (1-\alpha) \underline{\xi}_{i,\alpha} \right] + KF_i \right\} \tag{20}$$

s.t.

$$F_i = \bar{\psi}_i + \underline{\psi}_i \quad \forall i \tag{21}$$

$$\bar{\psi}_i = \left| y_i - g(x_i, w_{\bar{\alpha}}) \right| \quad \forall i \tag{22}$$

$$\underline{\psi}_i = \left| y_i - g(x_i, w_{\underline{\alpha}}) \right| \quad \forall i \tag{23}$$

$$\begin{cases} \bar{\psi}_i \ge 0 \quad \forall i \\ \underline{\psi}_i \ge 0 \quad \forall i \end{cases} \tag{24}$$

$$g(x_i, w_{\bar{\alpha}}) - \bar{\psi}_i \le y_i \quad \forall i \tag{25}$$

$$-g(x_i, w_{\bar{\alpha}}) - \bar{\psi}_i \le -y_i \quad \forall i \tag{26}$$

$$g(x_i, w_{\underline{\alpha}}) - \underline{\psi}_i \le y_i \quad \forall i \tag{27}$$

$$-g(x_i, w_{\underline{\alpha}}) - \underline{\psi}_i \le -y_i \quad \forall i \tag{28}$$

When the actual value lies in the PI, F_i denotes the width of the i^{th} PI. Otherwise, F_i can be quantified based on distances between the bounds and y_i, reflecting both the sharpness and OPOPI. By considering F_i, the overall performance of PIs can be directly optimized based on the efficient LP. F_i is defined as:

$$F_i = \begin{cases} W(x_i) + 2(g(x_i, w_{\underline{\alpha}}) - y_i) & y_i < g(x_i, w_{\underline{\alpha}}) \\ W(x_i) & y_i \in I_\alpha(x_i) \\ W(x_i) + 2(y_i - g(x_i, w_{\bar{\alpha}})) & y_i > g(x_i, w_{\bar{\alpha}}) \end{cases} \tag{29}$$

The conventional PIs quantify the nominal proportions of boundary quantiles based on (30) and (31).

$$\bar{\alpha} = 1 - \frac{1-\alpha}{2} \tag{30}$$

$$\underline{\alpha} = \frac{1-\alpha}{2} \tag{31}$$

To further improve the accuracy of boundary quantiles, ABQs are studied to optimize the bounds of PIs. The nominal proportion of upper quantile can be optimized by meta-heuristic algorithm adaptively, and the nominal proportion of lower quantile is quantified by:

$$\underline{\alpha}=\bar{\alpha}-\alpha \tag{32}$$

s.t.

$$\alpha\le\bar{\alpha}\le 1 \tag{33}$$

$$0\le\underline{\alpha}\le\alpha \tag{34}$$

III. Model Construction

In the proposed method, the training samples are clustered based on WMTSM. Then, with the clustering coefficients of training samples for CLP and composite optimization, CCNQR is performed. The training samples from the same cluster have the same C_i in (20). Particle swarm optimization (PSO) [34] is used twice to obtain the optimal coefficients. PSO is applied first to find the optimal λ_D, λ_T, and λ_ω of WMTSM. Considering both the optimization effectiveness and computation efficiency, the deterministic prediction error is used as the cost function. PSO is used again to optimize K and $\bar{\alpha}$ according to the reliability and overall performance of PIs in CCNQR. The major steps of the proposed method are as follows.

Step 1: initialize the coefficients of NQR and PSO, and set the confidence of PIs. Import and normalize the dataset for training and testing samples.

Step 2: quantify the correlations between outputs and variables of input vectors.

Step 3: for each iteration in the search space of PSO for optimal λ_D, λ_T, and λ_ω, based on WMTSM, the prediction error is utilized as the objective of the cost function.

Step 4: obtain the optimal coefficients and the clustering labels of training samples, and quantify the correlation coefficients of clusters as the weights of C_i in CLP.

Step 5: for each resolution in the search space of PSO to obtain the optimal K and nominal proportions of boundary quantiles for each cluster, based on the optimization function of CCNQR given in (10)-(13), (20)-(28), and (32)-(34), the quantification considering interval score and reliability is performed.

Step 6: based on the application result of CCNQR, the output weights of upper and lower quantiles in each cluster in the training process are calculated.

Step 7: by comparing the weighted distances between the inputs of testing samples and each cluster center, the labels of testing samples are obtained. Then, with the result of the training process, PIs can be quantified.

Remark 1: different from the high-fluctuating generation of single wind farm [17], [24], [35], the regional output is smoother [36]. Compared with the smoothing method which weights the historical regional wind power based on NWP [27], the proposed method uses data of NWP and historical power output for clustering. At the same time, it only uses the historical power observations as the input of the prediction model, less affected by NWP errors [11]. Unlike the conventional similarity analysis [16], in the hierarchical clustering method based on WMTSM, not only the similarity of the historical power and NWP, but also the dynamic correlation and weights of variables are considered.

Remark 2: different from LP [14], CLP considers the clustering coefficients which improve the accuracy of samples' utilization. Regarding the testing samples, the training samples of the same cluster have greater impact, while the samples from different clusters have less impact. Hence, instead of removing those low-impact samples, they are utilized with low correlation coefficients. The weights of training samples are adjusted based on the correlation coefficients. The CLP in the proposed method adopts an offline model, which can actually be used as a reference for the online model.

Remark 3: based on the criterion of interval score and considering $|ACE|$ in a reasonable range, the coefficient K in (20) is utilized to regulate different characteristics for the optimization of PIs. The sharpness and OPOPI are both considered in the composite optimization of CCNQR. This helps to fine-tune the PIs for better performance. Different from the conventional QR cost function that only considers the coverage accuracy of PIs [14], or the performance considering the reliability and sharpness [15], [37], the composite cost function of the proposed method directly and effectively quantifies the output weights by LP to obtain the optimal reliability and overall performance of PIs. Besides, ABQs can further improve the flexibility and robustness of PIs. The conventional values of K and $\bar{\alpha}$ can be set as the initial values to minimize the possibilities of low efficiency and local minimum in PSO.

IV. Case Studies

A. Introduction of Dataset

To fully verify the effectiveness of the proposed methodologies, two datasets are considered, which are given as follows.

1) Dataset 1: the wind power data of 20 wind farms located in the northeast of China with 15-min resolution covering the first half of 2019 and the corresponding wind speed data at 100 meters are studied. The data of the last 4 days in each month are used for testing and the data of the latest 11 days are used for training.

2) Dataset 2: the wind power data of 7 wind farms in Global Energy Forecasting Competition 2012 (GEFCom2012) with hourly resolution covering the second half of 2010 and the corresponding wind speed data at 10 meters are studied [38]. The data in June-August, September-October, and November-December are studied, respectively. The data of last 16 days are used for testing while the rest are set for training.

The wind speed at the time of wind power generation outage is set to be 0 in order to improve the accuracy and synchronization between the NWP data and wind farm outputs according to the outage plans. Historical power time series

with fewer zero output is selected to study the performance of PIs in each month. The results of different probabilistic prediction methods are then compared, and the datasets are used after normalization. The regional wind power as well as its variation is influenced by the nature of the wind farm itself, the different seasons, and the periods of time, i.e., recent observations of wind power output are more important than those observed earlier [27]. Besides, average offset (AO) is utilized to reveal the degree of OPOPI. The PIs with PINCs of 90% and 95% are obtained and evaluated, respectively.

B. Numerical Comparison of Clustering Methods

For numerical comparison of clustering-based deterministic predictions via ELM, the hourly-ahead prediction errors of the WMTSM-based method, *K*-means based method [39], and the conventional hierarchical clustering based method [30] for monthly regional wind power covering datasets 1 and 2 are shown in Fig. 2. Mean absolute error (MAE) and root mean squared error (RMSE) are used as the criteria of prediction performances [11]. It can be observed from Fig. 2 that the WMTSM-based method has the best accuracy.

C. Numerical Analysis of Coefficients

In this subsection, the data in January and June from dataset 1 and the data in September-October and November-December from dataset 2 are utilized to study the performance of PIs based on the weighting coefficients and the nominal proportions of upper quantiles.

The $-|ACE|$ and interval scores according to the nominal proportions of upper quantiles in ABQs and weighting coefficients in the training process are shown in Figs. 3-6 to reveal the performances of PIs. In these figures, the closer to zero the $-|ACE|$ or interval score, the better the reliability or overall performance of PIs. $\bar{\alpha}$ has resolutions of 0.25% and 0.125% with PINCs of 90% and 95%, respectively, where K has resolution of 0.0001. For the PIs based on dataset 1, $\bar{\alpha}$ ranges between α and 1, and K ranges from 0 to 0.004.

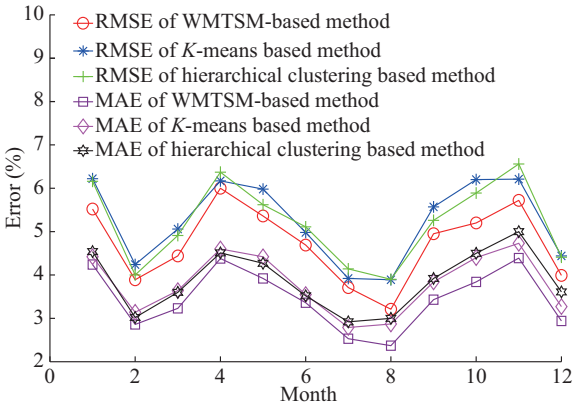

Fig. 2. Prediction errors of different clustering methods in each month covering datasets 1 and 2.

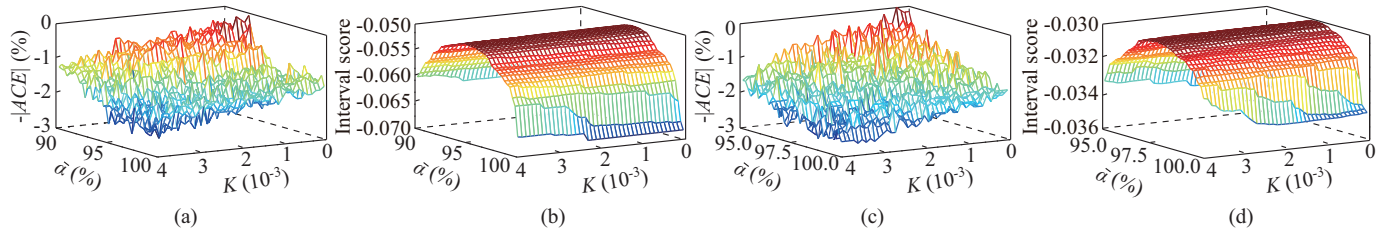

Fig. 3. Performances of PIs in January from dataset 1 with PINC of 90% and 95%. (a) Reliability with PINC of 90%. (b) Overall performance with PINC of 90%. (c) Reliability with PINC of 95%. (d) Overall performance with PINC of 95%.

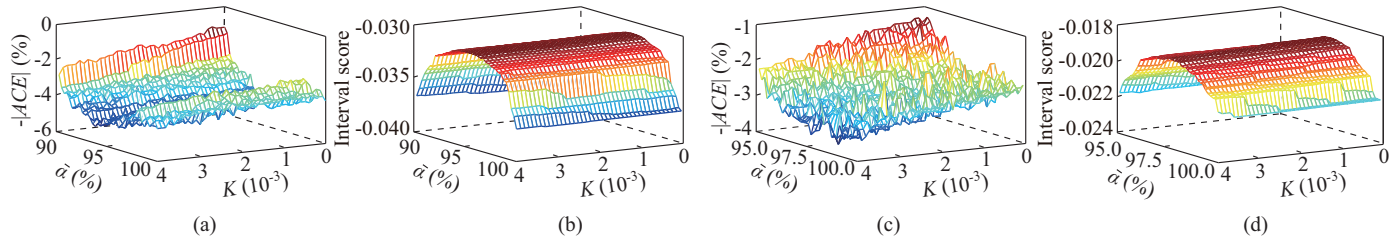

Fig. 4. Performances of PIs in June from dataset 1 with PINC of 90% and 95%. (a) Reliability with PINC of 90%. (b) Overall performance with PINC of 90%. (c) Reliability with PINC of 95%. (d) Overall performance with PINC of 95%.

Figures 3 and 4 show the performances of PIs with 1-hour look-ahead time. The optimal values of ($\bar{\alpha}$, K) are (95.25%, 0.0004), (97.375%, 0.0002), (95.5%, 0.0005), and (97.625%, 0.0007), respectively. In the conventional method [14], the proportion of upper quantile is set according to (30), and the weighting coefficient is set to be 0. Actually, the optimal coefficients are not the same as those in the conventional method. However, the values of conventional coefficients which are near the optimal values can be considered as the initial values of solutions to improve the computational efficiency. Thus, for the PIs based on dataset 2, the ranges of $\bar{\alpha}$ with PINC of 90% and of 95% are reduced to 93%-97% and 96.5%-98.5%, respectively, and K is reduced to 0-0.0015. Figures 5 and 6 illustrate the performances of PIs with 2-hour look-ahead time based on dataset 2, of which the optimal values of ($\bar{\alpha}$, K) are (94.75%, 0), (97%, 0.0002), (94.75%, 0.0002), and (97.25%, 0.0001), respectively. The numerical results of NQR and composite NQR (CNQR) are given in Tables I to IV. It can be remarked that CNQR has better forecasting performance.

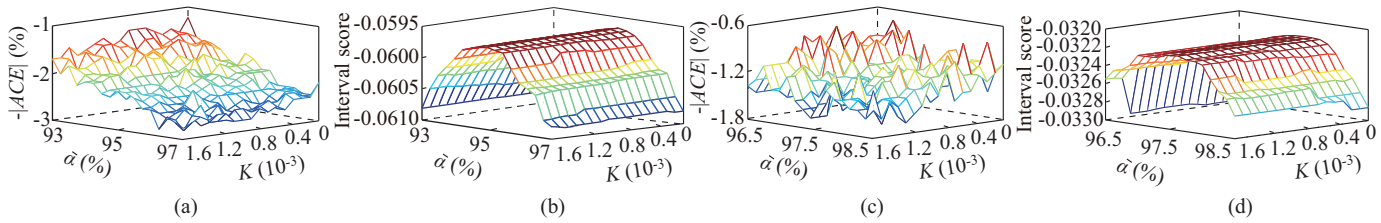

Fig. 5. Performances of PIs in September-October from dataset 2 with PINC of 90% and 95%. (a) Reliability with PINC of 90%. (b) Overall performance with PINC of 90%. (c) Reliability with PINC of 95%. (d) Overall performance with PINC of 95%.

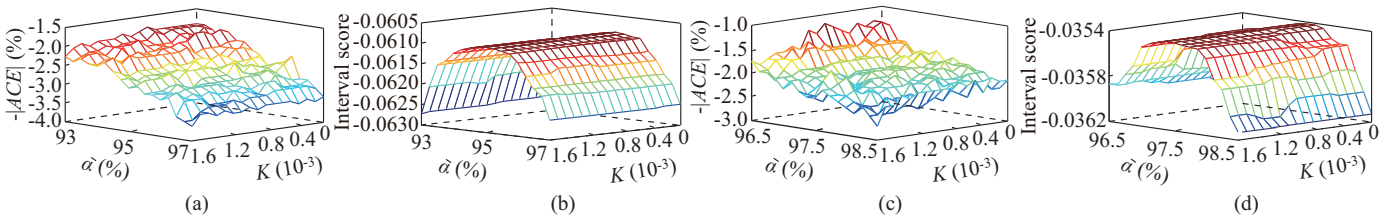

Fig. 6. Performances of PIs in November-December from dataset 2 with PINC of 90% and 95%. (a) Reliability with PINC of 90%. (b) Overall performance with PINC of 90%. (c) Reliability with PINC of 95%. (d) Overall performance with PINC of 95%.

TABLE I
COMPARISONS OF PIS IN JANUARY FROM DATASET 1

Method	PINC of 90%				PINC of 95%			
	PICP (%)	AW	AO	Score	PICP (%)	AW	AO	Score
NQR	91.93	0.2011	0.0241	–0.0480	93.75	0.2509	0.0176	–0.0295
CNQR	92.19	0.1994	0.0247	–0.0476	93.75	0.2471	0.0173	–0.0290

TABLE II
COMPARISONS OF PIS IN JUNE FROM DATASET 1

Method	PINC of 90%				PINC of 95%			
	PICP (%)	AW	AO	Score	PICP (%)	AW	AO	Score
NQR	95.05	0.2071	0.0257	–0.0465	96.88	0.2560	0.0317	–0.0296
CNQR	94.79	0.2038	0.0240	–0.0458	96.88	0.2514	0.0320	–0.0291

TABLE III
COMPARISONS OF PIS IN SEPTEMBER-OCTOBER FROM DATASET 2

Method	PINC of 90%				PINC of 95%			
	PICP (%)	AW	AO	Score	PICP (%)	AW	AO	Score
NQR	88.54	0.2368	0.0270	–0.0597	92.19	0.2697	0.0266	–0.0353
CNQR	89.58	0.2380	0.0283	–0.0597	92.97	0.2655	0.0307	–0.0352

TABLE IV
COMPARISONS OF PIS IN NOVEMBER-DECEMBER FROM DATASET 2

Method	PINC of 90%				PINC of 95%			
	PICP (%)	AW	AO	Score	PICP (%)	AW	AO	Score
NQR	86.72	0.2201	0.0207	–0.0550	91.93	0.2699	0.0139	–0.0315
CNQR	87.76	0.2191	0.0215	–0.0543	92.71	0.2710	0.0145	–0.0313

D. Numerical Comparison of Forecasting Performances

For the numerical analysis of the proposed method, the performances of BELM [15], CPPI [10], MLLP [11], CNQR, and hierarchical clustering based CNQR (HCNQR), are used for comparison, based on the data of January and June from dataset 1, and the data of September-October and November-December from dataset 2. The numerical results of dataset 1 with the 1-hour and 90-min look-ahead time are listed in Table V, while the numerical results of dataset 2 with 1-hour and 2-hour look-ahead time are listed in Table VI. CNQR and MLLP are both the nonparametric methods, so they have better robustness compared with the parametric methods. BELM and CPPI are the improved parametric methods based on Gaussian distribution. Based on hierarchical clustering, HCNQR selects the samples with high correlations for training, and removes the samples with low correlations. The numerical comparison between CNQR, HCNQR, and CCNQR shows that weighting training samples can further optimize the samples' utilization of CNQR-based nonparametric PIs. Consequently, the proposed method has the best forecasting performance among all the results shown in Tables V and VI. The cluster numbers of HCNQR and CCNQR are both set to be 4. A PC with Intel(R) Core(TM) i7-7700 CPU @ 2.8 GHz and 8 GB RAM is used for computations. The values of the computation time of HCNQR and CCNQR are less than 137 s and 175 s, respectively. As described in the previous analysis, since the optimal solution is not far from the conventional one, the prior knowledge for coefficients in the conventional QR can improve the computational efficiency and accuracy. That is, the initial variables of K and $\bar{a}$ are set to be 0 and according to (30), respectively, rather than be set according to random initial values in PSO. This can greatly reduce the number of iterations and the possibility of being trapped in local minimum of PSO.

To further verify the effectiveness of the proposed method in different periods, the numerical comparisons with different look-ahead time based on datasets 1 and 2 are presented

in Tables VII-X. The conventional PIs for the regional wind power based on deterministic prediction and Gaussian error distribution such as smoothing method [27], statistical upscaling method [24], and *K*-means clustering-based method [16], [37], [40] are used for comparison. In the smoothing method, the point prediction is quantified by weighting the STC coefficients based on the time interval and Euclidean distance of power observations. In the statistical upscaling method, the wind farms with both MAE and RMSE of less than 10% and the output correlations of more than 0.8 with regional output, are selected as representative wind farms. The number of clusters is set to be 7 considering the prediction performance by training. Furthermore, by considering the smoothing effect of regional wind power, the *K*-means clustering-based method is established with the regional wind power data. Among all these methods, the proposed method has the best performance of PIs. In most cases, both the *K*-means clustering-based method and the statistical upscaling method have better forecasting performances than the smoothing method. The smoothing method mainly relies on the wind speed of NWP to calculate the correlation and obtain similar power values of the training samples for weighting. This method is highly affected by the accuracy of NWP and the static relationship between the wind power and speed. Thus, its performance is much better when the NWP is accurate.

TABLE V
PERFORMANCES OF PIS BASED ON DATASET 1

Month	Method	PINC of 90%								PINC of 95%							
		1-hour (4-step ahead)				90-min (6-step ahead)				1-hour (4-step ahead)				90-min (6-step ahead)			
		PICP (%)	AW	AO	Score	PICP (%)	AW	AO	Score	PICP (%)	AW	AO	Score	PICP (%)	AW	AO	Score
Jan.	BELM	92.71	0.1957	0.0340	–0.0491	92.19	0.2561	0.0380	–0.0631	92.19	0.2372	0.0236	–0.0311	94.01	0.2973	0.0300	–0.0369
	CPPI	94.27	0.2085	0.0312	–0.0489	94.53	0.2757	0.0356	–0.0629	97.40	0.2559	0.0397	–0.0297	97.14	0.3307	0.0269	–0.0362
	MLLP	91.93	0.2026	0.0257	–0.0488	91.15	0.2633	0.0278	–0.0626	93.75	0.2412	0.0213	–0.0294	93.75	0.3146	0.0173	–0.0358
	CNQR	92.19	0.1994	0.0247	–0.0476	93.23	0.2691	0.0306	–0.0621	93.75	0.2471	0.0173	–0.0290	94.27	0.3027	0.0208	–0.0350
	HCNQR	91.15	0.2034	0.0205	–0.0480	90.63	0.2673	0.0233	–0.0622	94.27	0.2404	0.0213	–0.0285	93.49	0.2981	0.0232	–0.0359
	CCNQR	90.89	0.1862	0.0276	–0.0471	90.89	0.2530	0.0299	–0.0615	95.31	0.2490	0.0164	–0.0280	95.57	0.2751	0.0230	–0.0316
Jun.	BELM	85.94	0.1634	0.0332	–0.0513	92.97	0.2332	0.0417	–0.0584	92.19	0.1984	0.0368	–0.0313	92.97	0.2652	0.0434	–0.0387
	CPPI	87.24	0.1485	0.0390	–0.0496	87.50	0.1897	0.0398	–0.0578	90.89	0.1827	0.0322	–0.0300	91.15	0.2320	0.0355	–0.0358
	MLLP	94.53	0.2057	0.0291	–0.0475	95.57	0.2540	0.0149	–0.0568	96.88	0.2535	0.0084	–0.0295	96.88	0.3222	0.0152	–0.0379
	CNQR	94.79	0.2038	0.0240	–0.0458	92.45	0.2210	0.0393	–0.0561	96.88	0.2514	0.0320	–0.0291	96.61	0.2979	0.0349	–0.0345
	HCNQR	93.75	0.1874	0.0294	–0.0448	94.79	0.2494	0.0320	–0.0565	96.35	0.2493	0.0215	–0.0281	96.61	0.2997	0.0299	–0.0340
	CCNQR	92.71	0.1798	0.0293	–0.0445	92.71	0.2211	0.0322	–0.0536	95.05	0.2049	0.0271	–0.0259	95.57	0.2731	0.0278	–0.0322

TABLE VI
PERFORMANCES OF PIS BASED ON DATASET 2

Period	Method	PINC of 90%								PINC of 95%							
		1-hour (1-step ahead)				2-hour (2-step ahead)				1-hour (1-step ahead)				2-hour (2-step ahead)			
		PICP (%)	AW	AO	Score	PICP (%)	AW	AO	Score	PICP (%)	AW	AO	Score	PICP (%)	AW	AO	Score
Sept.-Oct.	BELM	86.98	0.1518	0.0288	–0.0454	86.64	0.2217	0.0363	–0.0640	91.15	0.1692	0.0313	–0.0280	91.67	0.2738	0.0414	–0.0412
	CPPI	86.98	0.1446	0.0292	–0.0441	88.80	0.2217	0.0421	–0.0632	92.71	0.1592	0.0276	–0.0240	93.49	0.2635	0.0431	–0.0376
	MLLP	87.76	0.1347	0.0187	–0.0375	87.50	0.2386	0.0273	–0.0613	91.93	0.1781	0.0137	–0.0229	94.27	0.2912	0.0220	–0.0362
	CNQR	88.54	0.1209	0.0257	–0.0360	89.58	0.2380	0.0283	–0.0597	92.71	0.1653	0.0167	–0.0214	92.97	0.2655	0.0307	–0.0352
	HCNQR	86.46	0.1212	0.0218	–0.0361	88.28	0.2282	0.0298	–0.0596	92.71	0.1610	0.0177	–0.0213	93.23	0.2717	0.0298	–0.0352
	CCNQR	90.10	0.1379	0.0191	–0.0351	90.36	0.2251	0.0315	–0.0572	93.75	0.1533	0.0199	–0.0203	95.05	0.2686	0.0302	–0.0328
Nov.-Dec.	BELM	87.50	0.1503	0.0155	–0.0378	91.15	0.2232	0.0348	–0.0570	94.01	0.1708	0.0230	–0.0244	92.97	0.2507	0.0356	–0.0350
	CPPI	94.27	0.1522	0.0247	–0.0361	95.31	0.2430	0.0390	–0.0559	96.61	0.1791	0.0327	–0.0223	97.66	0.2932	0.0458	–0.0336
	MLLP	87.76	0.1363	0.0214	–0.0351	87.76	0.2223	0.0314	–0.0556	93.49	0.1775	0.0202	0.0215	91.93	0.2649	0.0272	–0.0337
	CNQR	88.28	0.1343	0.0154	–0.0341	87.76	0.2191	0.0215	–0.0543	93.75	0.1581	0.0133	–0.0191	92.71	0.2710	0.0145	–0.0313
	HCNQR	88.80	0.1167	0.0170	–0.0310	86.72	0.2138	0.0198	–0.0533	93.94	0.1563	0.0145	–0.0194	93.23	0.2687	0.0161	–0.0312
	CCNQR	89.06	0.1135	0.0140	–0.0288	90.89	0.2063	0.0210	–0.0489	95.31	0.1543	0.0129	–0.0178	95.83	0.2615	0.0292	–0.0293

To reveal the result of proposed method with 1-hour look-ahead time, Fig. 7 demonstrates the PIs of wind power in January and April from dataset 1, while Fig. 8 depicts the PIs of wind power in September-October and November-December from dataset 2, where the values of wind power have been normalized. Those figures indicate that the PIs obtained by the proposed method have the good reliability and sharpness.

TABLE VII
NUMERICAL COMPARISONS WITH 1-HOUR LOOK-AHEAD TIME BASED ON DATASET 1

PINC (%)	Month	Smoothing method				Statistical upscaling method				*K*-means clustering-based method				Proposed method			
		PICP (%)	AW	AO	Score	PICP (%)	AW	AO	Score	PICP	AW	AO	Score	PICP (%)	AW	AO	Score
90	Jan.	100.00	0.4498	None	–0.0900	94.27	0.2366	0.0320	–0.0546	87.50	0.1765	0.0473	–0.0590	90.89	0.1862	0.0276	–0.0471
	Feb.	98.96	0.4590	0.2410	–0.1018	94.27	0.1807	0.0245	–0.0418	86.46	0.1205	0.0231	–0.0366	89.06	0.1389	0.0170	–0.0352
	Mar.	92.71	0.4084	0.0965	–0.1098	93.75	0.1767	0.0404	–0.0454	85.68	0.1301	0.0348	–0.0459	89.84	0.1569	0.0247	–0.0414
	Apr.	84.64	0.4140	0.0449	–0.1104	83.85	0.2106	0.0400	–0.0679	85.42	0.1649	0.0449	–0.0592	90.36	0.2082	0.0301	–0.0529
	May	96.09	0.4430	0.0633	–0.0985	86.72	0.3138	0.0466	–0.0875	86.20	0.1737	0.0399	–0.0568	89.84	0.1915	0.0247	–0.0483
	Jun.	67.19	0.0896	0.0449	–0.0769	83.07	0.1342	0.0344	–0.0501	85.94	0.1436	0.0321	–0.0468	92.71	0.1798	0.0293	–0.0445
95	Jan.	100.00	0.5936	None	–0.0505	97.14	0.2821	0.0369	–0.0324	91.93	0.2145	0.0434	–0.0355	95.31	0.2490	0.0164	–0.0280
	Feb.	100.00	0.4832	None	–0.0483	97.40	0.2172	0.0258	–0.0244	91.41	0.1444	0.0272	–0.0238	93.23	0.1802	0.0147	–0.0220
	Mar.	99.48	0.4943	0.0390	–0.0502	95.57	0.2093	0.0364	–0.0274	89.58	0.1535	0.0369	–0.0307	94.53	0.2050	0.0196	–0.0248
	Apr.	96.61	0.5196	0.0805	–0.0629	90.36	0.2528	0.0382	–0.0400	91.41	0.1982	0.0434	–0.0347	94.79	0.2407	0.0365	–0.0317
	May	96.88	0.4943	0.0433	–0.0548	94.45	0.3743	0.0405	–0.0497	90.10	0.2035	0.0363	–0.0347	95.31	0.2520	0.0172	–0.0284
	Jun.	82.03	0.1241	0.0375	–0.0393	89.06	0.1601	0.0347	–0.0312	92.19	0.1772	0.0299	–0.0270	95.05	0.2049	0.0271	–0.0259

TABLE VIII
NUMERICAL COMPARISONS WITH 90-MIN LOOK-AHEAD TIME BASED ON DATASET 1

PINC (%)	Month	Smoothing method				Statistical upscaling method				*K*-means clustering-based method				Proposed method			
		PICP (%)	AW	AO	Score	PICP (%)	AW	AO	Score	PICP (%)	AW	AO	Score	PICP (%)	AW	AO	Score
90	Jan.	100.00	0.4636	None	–0.0873	94.01	0.2950	0.0407	–0.0688	86.72	0.2283	0.0653	–0.0803	90.89	0.2530	0.0299	–0.0615
	Feb.	97.40	0.4608	0.0883	–0.1014	96.05	0.2463	0.0293	–0.0538	86.72	0.1823	0.0330	–0.0522	89.84	0.1998	0.0207	–0.0484
	Mar.	93.23	0.4041	0.0755	–0.1013	93.75	0.2368	0.0498	–0.0598	84.90	0.1790	0.0530	–0.0678	90.63	0.1941	0.0204	–0.0453
	Apr.	84.64	0.4401	0.0632	–0.1269	81.77	0.2786	0.0476	–0.0905	83.33	0.2213	0.0522	–0.0791	90.10	0.2287	0.0338	–0.0591
	May	89.32	0.4390	0.0731	–0.1190	86.46	0.3524	0.0535	–0.0994	83.85	0.2247	0.0524	–0.0788	90.36	0.2361	0.0280	–0.0580
	Jun.	62.76	0.0922	0.0426	–0.0819	86.20	0.1734	0.0438	–0.0589	86.98	0.1917	0.0344	–0.0574	92.71	0.2211	0.0322	–0.0536
95	Jan.	100.00	0.5774	None	–0.0577	96.61	0.3526	0.0383	–0.0404	91.93	0.2737	0.0539	–0.0448	95.57	0.2751	0.0230	–0.0316
	Feb.	100.00	0.5072	None	–0.0507	98.18	0.2912	0.0349	–0.0317	92.45	0.2173	0.0284	–0.0303	94.27	0.2665	0.0140	–0.0298
	Mar.	95.83	0.4242	0.0547	–0.0515	95.83	0.2799	0.0491	–0.0362	89.06	0.2095	0.0567	–0.0457	95.05	0.2175	0.0207	–0.0258
	Apr.	88.54	0.5143	0.0459	–0.0724	89.32	0.3299	0.0472	–0.0532	89.58	0.2612	0.0589	–0.0506	93.49	0.2637	0.0331	–0.0350
	May	93.49	0.4948	0.0251	–0.0560	91.15	0.4211	0.0419	–0.0569	90.10	0.2687	0.0537	–0.0481	95.83	0.3205	0.0317	–0.0373
	Jun.	84.38	0.1513	0.0473	–0.0447	91.41	0.2068	0.0505	–0.0381	92.45	0.2324	0.0342	–0.0336	95.57	0.2731	0.0278	–0.0322

TABLE IX
NUMERICAL COMPARISONS WITH 1-HOUR LOOK-AHEAD TIME BASED ON DATASET 2

PINC (%)	Period	Smoothing method				Statistical upscaling method				*K*-means clustering-based method				Proposed method			
		PICP (%)	AW	AO	Score	PICP (%)	AW	AO	Score	PICP (%)	AW	AO	Score	PICP (%)	AW	AO	Score
90	Jul.-Aug.	97.66	0.3178	0.0707	–0.0702	85.94	0.1994	0.0394	–0.0620	93.23	0.1105	0.0168	–0.0267	91.41	0.1139	0.0112	–0.0266
	Sept.-Oct.	97.40	0.3334	0.0231	–0.0691	88.80	0.2242	0.0444	–0.0648	85.68	0.1184	0.0311	–0.0415	90.10	0.1379	0.0191	–0.0351
	Nov.-Dec.	97.92	0.3343	0.0418	–0.0703	92.45	0.2264	0.0224	–0.0521	93.23	0.1144	0.0246	–0.0296	89.06	0.1135	0.0140	–0.0288
95	Jul.-Aug.	98.44	0.3804	0.0472	–0.0410	90.36	0.2356	0.0315	–0.0357	96.35	0.1311	0.0183	–0.0158	95.05	0.1404	0.0074	–0.0155
	Sept.-Oct.	99.74	0.3990	0.0055	–0.0400	92.71	0.2655	0.0421	–0.0388	91.41	0.1425	0.0332	–0.0247	94.01	0.1563	0.0188	–0.0201
	Nov.-Dec.	99.22	0.4285	0.0506	–0.0444	95.51	0.2700	0.0204	–0.0298	96.35	0.1380	0.0330	–0.0183	95.31	0.1543	0.0129	–0.0178

V. CONCLUSION

In this paper, a novel probabilistic prediction method based on CCNQR is proposed for very short-term PIs of regional wind power, which implements the following four tasks. Firstly, WMTSM clustering the samples by considering the static difference, dynamic difference, meteorological difference and the importance of variables is verified by numerical comparison of deterministic predictions. Secondly, CNQR considering reliability, sharpness, and OPOPI for the performance improvement of PIs is studied, while the ABQs are studied to improve the flexibility and robustness of PIs.

TABLE X
NUMERICAL COMPARISONS WITH 2-HOUR LOOK-AHEAD TIME BASED ON DATASET 2

PINC (%)	Period	Smoothing method				Statistical upscaling method				*K*-means clustering-based method				Proposed method			
		PICP (%)	AW	AO	Score	PICP (%)	AW	AO	Score	PICP (%)	AW	AO	Score	PICP (%)	AW	AO	Score
90	Jul.-Aug.	94.53	0.3254	0.0589	–0.0780	86.98	0.2486	0.0474	–0.0744	92.97	0.1907	0.0342	–0.0478	91.67	0.1202	0.0121	–0.0281
	Sept.-Oct.	95.31	0.3782	0.0359	–0.0824	88.54	0.2839	0.0479	–0.0787	88.02	0.2134	0.0524	–0.0678	90.36	0.2251	0.0315	–0.0572
	Nov.-Dec.	98.44	0.4275	0.0939	–0.0914	94.53	0.2995	0.0556	–0.0721	92.97	0.2069	0.0303	–0.0499	90.89	0.2063	0.0210	–0.0489
95	Jul.-Aug.	96.88	0.3680	0.0652	–0.0450	91.67	0.2970	0.0412	–0.0434	96.35	0.2266	0.0405	–0.0286	95.05	0.1495	0.0070	–0.0165
	Sept.-Oct.	98.44	0.4110	0.0494	–0.0442	93.23	0.3379	0.0471	–0.0466	91.15	0.2545	0.0440	–0.0410	95.05	0.2686	0.0302	–0.0328
	Nov.-Dec.	99.74	0.6084	0.0001	–0.0608	96.35	0.3555	0.0474	–0.0425	96.88	0.2608	0.0312	–0.0300	95.83	0.2615	0.0292	–0.0293

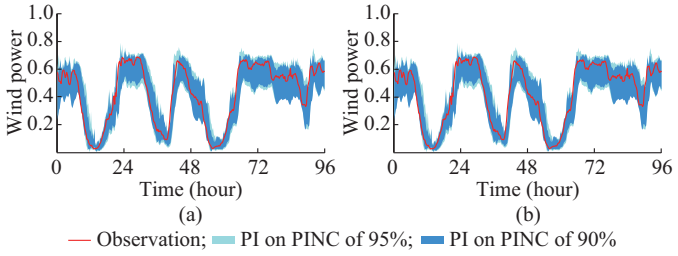

Fig. 7. PIs of wind power in January and April from dataset 1. (a) January. (b) April.

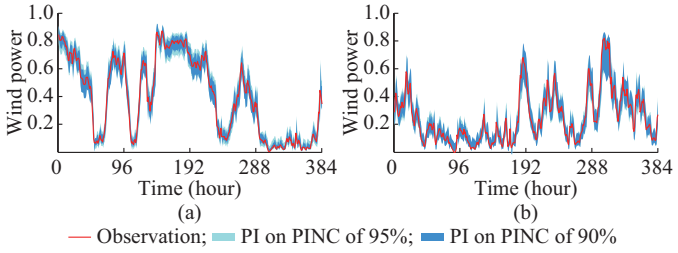

Fig. 8. PIs of wind power in September-October and November-December from dataset 2. (a) September-October. (b) November-December.

As verified by the analysis of coefficients and numerical comparisons with different PINCs and look-ahead time, the composite optimization and ABQs improve the forecasting performance. Thirdly, with the result of clustering, the CLP for each cluster is quantified, which can improve the accuracy of samples' utilization, and further enhance the performance of CNQR. Finally, the numerical comparisons with existing methods for different PINCs and look-ahead time demonstrate the effectiveness of the proposed method.

The future work may focus on the advanced method of dynamic analysis, which can accurately describe the characteristics of wind power time series. Besides, the analysis of STC can also be utilized to improve the performance of PIs for regional output.

REFERENCES

[1] B. Mohandes, M. S. E. Moursi, N. Hatziargyriou *et al.*, "A review of power system flexibility with high penetration of renewables," *IEEE Transactions on Power Systems*, vol. 34, no. 4, pp. 3140-3155, Jul. 2019.

[2] B. Liu, K. Meng, Z. Dong *et al.*, "Marginal bottleneck identification in power system considering correlated wind power prediction errors," *Journal of Modern Power Systems and Clean Energy*, vol. 8, no. 1, pp. 187-192, Jan. 2020.

[3] L. Ge, Y. Xian, J. Yan *et al.*, "A hybrid model for short-term PV output forecasting based on PCA-GWO-GRNN," *Journal of Modern Power Systems and Clean Energy*, vol. 8, no. 6, pp. 1268-1275, Nov. 2020.

[4] Y. Wang, Y. Sun, V. Dinavhi *et al.*, "Robust forecasting-aided state estimation for power system against uncertainties," *IEEE Transactions on Power Systems*, vol. 35, no. 1, pp. 691-702, Aug. 2020.

[5] A. Cerejo, S. J. P. S. Mariano, P. M. S. Carvalh *et al.*, "Hydro-wind optimal operation for Joint bidding in day-ahead market: storage efficiency and impact of wind forecasting uncertainty," *Journal of Modern Power Systems and Clean Energy*, vol. 8, no. 1, pp. 142-149, Jan. 2020.

[6] Y. Zhao, L. Ye, P. Pinson *et al.*, "Correlation-constrained and sparsity-controlled vector autoregressive model for spatio-temporal wind power forecasting," *IEEE Transactions on Power Systems*, vol. 33, no. 5, pp. 5029-5040, Sept. 2018.

[7] Y. Lin, M. Yang, C. Wan *et al.*, "A multi-model combination approach for probabilistic wind power forecasting," *IEEE Transactions on Sustainable Energy*, vol. 10, no. 1, pp. 226-237, Jan. 2019.

[8] J. T. G. Hwang and A. Ding, "Prediction intervals for artificial neural networks," *Journal of the American Statistical Association*, vol. 92, no. 438, pp. 748-757, Jun. 1997.

[9] Z. Wang, W. Wang, C. Liu *et al.*, "Forecasted scenarios of regional wind farms based on regular vine copulas," *Journal of Modern Power Systems and Clean Energy*, vol. 8, no. 1, pp. 77-85, Jan. 2020.

[10] Y. Sun, P. Wang, S. Zhai *et al.*, "Ultra short-term probability prediction of wind power based on LSTM network and condition normal distribution," *Wind Energy*, vol. 23, no. 2, pp. 63-76, Oct. 2019.

[11] C. Wan, Z. Xu, P. Pinson *et al.*, "Probabilistic forecasting of wind power generation using extreme learning machine," *IEEE Transactions on Power Systems*, vol. 29, no. 3, pp. 1033-1044, May 2014.

[12] C. Wan, Z. Xu, P. Pinson *et al.*, "Direct interval forecasting of wind power," *IEEE Transactions on Power Systems*, vol. 28, no. 4, pp. 4877-4878, Nov. 2013.

[13] R. Koenker and G. Bassett, "Regression quantiles," *Econometrica*, vol. 46, no. 1, pp. 33-50, Jan. 1978.

[14] C. Wan, J. Lin, J. Wang *et al.*, "Direct quantile regression for nonparametric probabilistic forecasting of wind power generation," *IEEE Transactions on Power Systems*, vol. 32, no. 4, pp. 2767-2778, Jul. 2016.

[15] C. Wan, J. Wang, J. Lin *et al.*, "Nonparametric prediction intervals of wind power via linear programming," *IEEE Transactions on Power Systems*, vol. 33, no. 1, pp. 1074-1076, Jan. 2018.

[16] A. Xu, T. Yang, J. Ji *et al.*, "Application of cluster analysis in short-term wind forecasting model," *The Journal of Engineering*, vol. 2019, no. 9, pp. 5423-5426, Apr. 2019.

[17] Q. Xu, D. He, N. Zhang *et al.*, "A short-term wind power forecasting approach with adjustment of numerical weather prediction input by data mining," *IEEE Transactions on Sustainable Energy*, vol. 6, no. 4, pp. 1283-1291, Jun. 2015.

[18] G. Sideratos and N. Hatziargyriou, "Probabilistic wind power forecasting using radial basis function neural networks," *IEEE Transactions on Power Systems*, vol 27, no. 4, pp. 1788-1796, Nov. 2012.

[19] G. Sideratos and N. Hatziargyriou, "A distributed memory RBF-based model for variable generation forecasting," *International Journal of Electrical Power & Energy Systems*, vol. 120, pp. 106041, Sept. 2020.

[20] G. Sideratos and N. Hatziargyriou, "An advanced statistical method for wind power forecasting," *IEEE Transactions on Power Systems*, vol. 22, no. 1, pp. 258-265, Mar. 2007.

[21] G. Sideratos, A. Ikonomopoulos, and N. Hatziargyriou, "A novel

fuzzy-based ensemble model for load forecasting using hybrid deep neural networks," *Electric Power Systems Research*, vol. 178, p. 106025, Jan. 2020.
[22] M. Marinelli, P. Maul, A. N. Hahmann *et al.*, "Wind and photovoltaic large-scale regional models for hourly production evaluation," *IEEE Transactions on Sustainable Energy*, vol. 6, no. 3, pp. 916-923, Sept. 2015.
[23] M. B. Ozkan and P. Karagoz, "A novel wind power forecast model: statistical hybrid wind power forecast technique (SHWIP)," *IEEE Transactions on Industrial Informatics*, vol. 11, no. 2, pp. 375-387, Apr. 2015.
[24] M. B. Ozkan and P. Karagoz, "Data mining-based upscaling approach for regional wind power forecasting: regional statistical hybrid wind power forecast technique (regional SHWIP)," *IEEE Access*, vol. 7, pp. 171790-171800, Nov. 2019.
[25] Q. Zhu, J. Chen, D. Shi *et al.*, "Learning temporal and spatial correlations jointly: a unified framework for wind speed prediction," *IEEE Transactions on Sustainable Energy*, vol. 11, no. 1, pp. 509-523, Sept. 2015.
[26] M. He, L. Yang, J. Zhang *et al.*, "A spatio-temporal analysis approach for short-term forecast of wind farm generation," *IEEE Transactions on Power Systems*, vol. 29, no. 4, pp. 1611-1622, Jul. 2014.
[27] M. G. Lobo and I. Sanchez, "Regional wind power forecasting based on smoothing techniques, with application to the Spanish peninsular system," *IEEE Transactions on Power Systems*, vol. 27, no. 4, pp. 1990-1997, Nov. 2012.
[28] Q. Liang, Y. Xiong, and K. Liu, "Weather division-based wind power forecasting model with feature selection," *IET Renewable Power Generation*, vol. 13, no. 16, pp. 3050-3060, Oct. 2019.
[29] W. Xie, R. Han, and W. Zhou, "Time series classification based on triadic time series motifs," *International Journal of Modern Physics A*, vol. 33, no. 21, pp. 1-14, Jan. 2019.
[30] G. Karypis, E. Han, and V. Kumar, "Chameleon: hierarchical clustering using dynamic modeling," *IEEE Computer Society*, vol. 32, no. 8, pp. 68-75, Sept. 1999.
[31] C. Spearman, "The proof and measurement of association between two things," *International Journal of Epidemiology*, vol. 39, no. 5, pp. 1137-1150, Oct. 2010.
[32] H. Wang and B. Zou, "Probabilistic computational model for correlated wind speed, solar irradiation, and load using Bayesian network," *IEEE Access*, vol. 8, pp. 51653-51663, Mar. 2020.
[33] C. Wan, Z. Xu, P. Pinson *et al.*, "Optimal prediction intervals of wind power generation," *IEEE Transactions on Power Systems*, vol. 29, no. 3, pp. 1166-1174, May 2014.
[34] J. Kennedy and R. C. Eberhart, "Particle swarm optimization," in *Proceedings of 1995 IEEE International Conference on Neural Networks*, Perth, Australia, Nov. 1995, pp. 1942-1948.
[35] M. Yang, X. Chen, and B. Huang, "Ultra-short-term multi-step wind power prediction based on fractal scaling factor transformation," *Journal of Renewable and Sustainable Energy*, vol. 10, no. 5, pp. 1-17, Oct. 2018.
[36] M. Yang, R. Zhang, Y. Cui *et al.*, "Investigating the wind power smoothing effect using set pair analysis," *IEEE Transactions on Sustainable Energy*, vol. 11, no. 3, pp. 1161-1172, Jul. 2020.
[37] L. Ye, C. Zhang, Y. Tang *et al.*, "Hierarchical model predictive control strategy based on dynamic active power dispatch for wind power cluster integration," *IEEE Transactions on Power Systems*, vol. 34, no. 6, pp. 4617-4629, Nov. 2019.
[38] T. Hong, P. Pinson, and S. Fan, "Global energy forecasting competition 2012," *International Journal of Forecasting*, vol. 30, no. 2, pp. 351-363, Apr.-Jun. 2014.
[39] X. Huang, Y. Ye, and H. Zhang, "Extensions of K means-type algorithms: a new clustering framework by integrating intracluster compactness and intercluster separation," *IEEE Transactions on Systems, Man, and Cybernetics: Systems*, vol. 25, no. 8, pp. 1433-1446, Aug. 2014.
[40] M. Yang, C. Shi, and H. Liu, "Day-ahead wind power forecasting based on the clustering of equivalent power curves," *Energy*, vol. 218, p. 119515, Mar. 2021.

Yan Zhou is currently pursuing the Ph. D. degree in electrical engineering from Hohai University, Nanjing, China. His research interests include power big data analysis, machine learning, power system operation optimization, and renewable energy generation forecasting.

Yonghui Sun received the Ph. D. degree in electrical engineering from the City University of Hong Kong, Hong Kong, China, in 2010. He is currently a Professor with the College of Energy and Electrical Engineering, Hohai University, Nanjing, China. His research interests include stability analysis and control of power systems, optimal planning and operation of the integrated energy system, optimization algorithms, and data analysis.

Sen Wang is currently pursuing the Ph. D. degree in electrical engineering with Hohai University, Nanjing, China. His research interests include power big data analysis, renewable energy grid-connected control, power system operation optimization, and renewable energy generation forecasting.

Rabea Jamil Mahfoud received the Ph. D. degree in electrical engineering from Hohai University, Nanjing, China, in 2020. His current research interests include optimal operation and planning of power systems, optimization algorithms, and data analysis.

Hassan Haes Alhelou is currently a Faculty Member with Tishreen University, Lattakia, Syria. He was a recipient of the Outstanding Reviewer Award from Energy Conversion and Management Journal in 2016, ISA Transactions Journal in 2018, Applied Energy Journal in 2019, and many other awards. He is included in the year 2018 and 2019 Publons list of the Top 1% Best Reviewer and Researchers in the field of engineering. His major research interests include, power system dynamics, power system operation and control, dynamic state estimation, frequency control, smart grids, microgrids, demand response, load shedding, and power system protection.

Nikos Hatziargyriou is a Professor in power systems at the National Technical University of Athens, Athens, Greece. He has over 10-year industrial experience as Chairman and CEO of the Hellenic Distribution Network Operator (HEDNO), Athens, Greece. He was Chair and Vice-chair of the EU Technology and Innovation Platform on Smart Networks for Energy Transition (ETIP-SNET) representing E. DSO. He is Life Fellow Member of IEEE, past Chair of the Power System Dynamic Performance Committee (PSDPC) and currently Editor in Chief of the IEEE Transactions on Power Systems. He is included in the 2016, 2017, and 2019 Thomson Reuters lists of the top 1% Most Cited Researchers and he is 2020 Globe Energy Prize laureate. His research interests include smart grids, microgrids, distributed and renewable energy sources, and power system security.

Pierluigi Siano received the M.Sc. degree in electronic engineering and the Ph. D. degree in information and electrical engineering from the University of Salerno, Salerno, Italy, in 2001 and 2006, respectively. He is currently a Professor and the Scientific Director of the Smart Grids and Smart Cities Laboratory, Department of Management and Innovation Systems, University of Salerno. In 2019 and 2020, he received award as a Highly Cited Researcher from the ISI Web of Science Group. He has been the Chair of the IES TC on Smart Grids. He is an Editor of the Power and Energy Society Section of IEEE Access, IEEE Transactions on Industrial Informatics, IEEE Transactions on Industrial Electronics, IEEE Open Journal of the Industrial Electronics Society, IET Smart Grid, and IET Renewable Power Generation. His research interests include demand response, energy management, integration of distributed energy resources in smart grids, electricity market, and planning and management of power systems.